Proceedings of the World Congress on Engineering 2014 Vol II,
WCE 2014, July 2 - 4, 2014, London, U.K.

Mixed FEM-BEM Formulations Applied to Soil-Structure Interaction Problems

Dimas Betioli Ribeiro and João Batista de Paiva

Abstract—**The objective of this paper is to present formulations developed for soil-building interaction analysis, including foundations. The soil is modeled with the boundary element method (BEM) as a layered solid which may be finite for the vertical direction, but is always infinite for radial directions. Beams, collums and piles are modeled with the finite element method (FEM) using one dimensional elements. Slabs and rafts are also modeled with the FEM, but with two dimensional elements. The analysis is static and all materials are considered homogeneous, isotropic, elastic and with linear behavior.**

Index Terms—**boundary elements, finite elements, soil-structure interaction.**

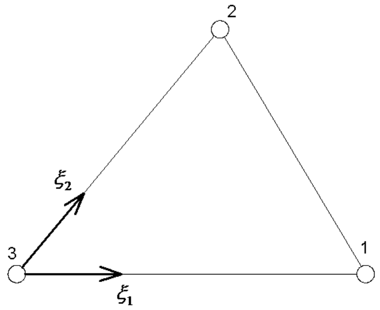

Fig. 1. Triangular boundary element.

I. INTRODUCTION

The construction of buildings involve complex soil-structure interaction effects that require previous studies to be correctly considered in the project. The basis of these studies has to be chosen among many options available and each one of them implies on advantages and disadvantages, as described below.

When possible, a good choice is to employ analytical methods. When correctly programmed they give trustful results in little processing time. In reference [1], for example, a solution is presented for an axially loaded pile with a rectangular cross section and immersed in a layered isotropic domain. The main disadvantage of these solutions is that they suit only specific situations, so many researches keep developing new ones to include new problems. Other works that may be cited are [2], [3].

If analytical solutions cannot be used, one alternative could be a numerical approach. The developments [4] of the numerical methods in the latter years and its versatility made them attractive to many researchers. The finite element method (FEM) is still popular [5], [6], [7], [8], however has some disadvantages when compared to other options such as the boundary element method (BEM). The FEM require the discretization of the domain, which has to be simulated as infinite in most soil-structure interaction problems. This implies on a high number of elements, leading to a large and sometimes impracticable processing time.

It becomes more viable solving these problems with the BEM, once only the boundary of the domains involved is discretized. This allows reducing the problem dimension, implying on less processing time. This advantage is explored in several works [9], [10], [11], [12], [13], [14], [15], [16] and new developments are making the BEM even more attractive to future applications. One is simulating non-homogeneous domains using an alternative multi-domain BEM technique [17], another is using mapping functions to make boundary elements infinite [18].

The objective of this paper is to present a formulation for building-soil interaction analysis that uses recent developments accomplished by the authors in references [17], [18]. The proposed formulation is applied into two examples to show all functionalities of the proposed formulation, considering a piled raft and a complete building interacting with a layered soil. The results obtained may be considered coherent. Finally, it is concluded that the presented formulation may be considered a practical and attractive alternative in the field of soil-structure interaction simulation.

Manuscript received March 21, 2014; revised March 25, 2014. This work was supported by the research council FAPESP.

D. B. Ribeiro is with the Department of Structural and Geotechnical Engineering, Polytechnic School of the University of São Paulo, São Paulo, SP, 05508-070 Brazil e-mail: dimas.ribeiro@usp.br.

J. B. Paiva is with the School of Engineering of São Carlos, University of São Paulo, São Carlos, SP, 13566-590 Brazil e-mail: paiva@sc.usp.br.

II. BOUNDARY ELEMENT FORMULATION

The equilibrium of a solid body can be represented by a boundary integral equation called the Somigliana Identity, which for homogeneous, isotropic and linear-elastic domains is

$$\begin{aligned} c_{ij}(y)\,u_j(y) + \int_\Gamma p^*_{ij}(x,y)\,u_j(x)\,d\Gamma(x) \\ = \int_\Gamma u^*_{ij}(x,y)\,p_j(x)\,d\Gamma(x) \end{aligned} \tag{1}$$

Equation (1) is written for a source point y at the boundary, where the displacement is $u_j(y)$. The constant c_{ij} depends on the Poisson ratio and the boundary geometry at y, as pointed out in reference [20]. The field point x goes through the whole boundary Γ, where displacements are $u_j(x)$ and tractions are $p_j(x)$. The integral kernels $u^*_{ij}(x,y)$ and $p^*_{ij}(x,y)$ are Kelvin three-dimensional fundamental solutions for displacements and tractions, respectively. Kernel $u^*_{ij}(x,y)$ has order $1/r$ and kernel $p^*_{ij}(x,y)$ order $1/r^2$, where $r = |x-y|$, so the integrals have singularity problems when x approaches y. Therefore the stronger singular integral, over the traction kernel, has to be defined in terms of a Cauchy Principal Value (CPV).

To solve Equation (1) numerically, the boundary is divided into regions within which displacements and tractions are approximated by known shape functions. Here these regions are of two types, finite boundary elements (BEs) and infinite boundary elements (IBEs). The BEs employed are triangular, as shown in Figure 1 with the local system of coordinates, $\xi_1\xi_2$, and the local node numbering. The following approximations are used for this BE:

$$u_j = \sum_{k=1}^{3} N^k u_j^k, \quad p_j = \sum_{k=1}^{3} N^k p_j^k \tag{2}$$

Equation (2) relates the boundary values u_j and p_j to the nodal values of the BE. The BEs have 3 nodes and for each node there are three components of displacement u_j^k and traction p_j^k. The shape functions N^k used for these approximations are

$$N^1 = \xi_1, \quad N^2 = \xi_2, \quad N^3 = 1 - \xi_1 - \xi_2 \tag{3}$$

The same shape functions are used to approximate the boundary geometry:

$$x_j = \sum_{k=1}^{3} N^k x_j^k \tag{4}$$

where x_j^k are the node coordinates. The same functions are also used to interpolate displacements and tractions for the IBEs:

$$u_j = \sum_{k=1}^{Np} N^k u_j^k, \quad p_j = \sum_{k=1}^{Np} N^k p_j^k \tag{5}$$

Each IBE has Np nodes and not the 3 that the BEs have. The IBE geometry, on the other hand, is approximated by special mapping functions.

By substituting Equations (2) and (5) in (1), Equation (6) is obtained:

$$\begin{aligned} c_{ij}u_j + \sum_{e=1}^{N_{BE}} \left\{ \sum_{k=1}^{3} \left[\Delta p_{ij}^{ek} u_j^k \right] \right\} + \sum_{e=1}^{N_{IBE}} \left\{ \sum_{k=1}^{Np} \left[\Delta^\infty p_{ij}^{ek} u_j^k \right] \right\} \\ = \sum_{e=1}^{N_{BE}} \left\{ \sum_{k=1}^{3} \left[\Delta u_{ij}^{ek} p_j^k \right] \right\} + \sum_{e=1}^{N_{IBE}} \left\{ \sum_{k=1}^{Np} \left[\Delta^\infty u_{ij}^{ek} p_j^k \right] \right\} \end{aligned} \tag{6}$$

N_{BE} is the number of BEs and N_{IBE} is the number of IBEs. For BEs:

$$\Delta p_{ij}^{ek} = \int_{\gamma_e} |J| \, N^k p_{ij}^* (x, y) \, d\gamma_e \tag{7}$$

$$\Delta u_{ij}^{ek} = \int_{\gamma_e} |J| \, N^k u_{ij}^* (x, y) \, d\gamma_e \tag{8}$$

In Equations (7) and (8), γ_e represents the domain of element e in the local coordinate system and the global system of coordinates is transformed to the local one by the Jacobian $|J| = 2A$, where A is the element area in the global system. On the other hand, for IBEs:

$$\Delta^\infty p_{ij}^{ek} = \int_{\gamma_e} |^\infty J| \, N^k p_{ij}^* (x, y) \, d\gamma_e \tag{9}$$

$$\Delta^\infty u_{ij}^{ek} = \int_{\gamma_e} |^\infty J| \, N^k u_{ij}^* (x, y) \, d\gamma_e \tag{10}$$

Equations (9) and (10) are analogous to (7) and (8). Integrals of Equations (7), (8), (9) and (10) are calculated by standard BEM techniques. Non-singular integrals are evaluated numerically by using integration points. The singular ones, on the other hand, are evaluated by the technique presented in reference [19]. Finally, the free term c_{ij} may be obtained by rigid body motions. Writing Equation (6) for all boundary nodes leads to the following system:

$$\Delta p \cdot u = \Delta u \cdot p \tag{11}$$

The Δp_{ij}^{ek} and $\Delta^\infty p_{ij}^{ek}$ element contributions, including the free term c_{ij}, are assembled into matrix Δp, while Δu_{ij}^{ek} and $\Delta^\infty u_{ij}^{ek}$ contributions are assembled into matrix Δu. Vectors u and p contain all boundary displacements and tractions, respectively. Reorganizing this system so as to separate the known boundary values from the unknown yields a system of equations whose solution is all the unknown boundary values.

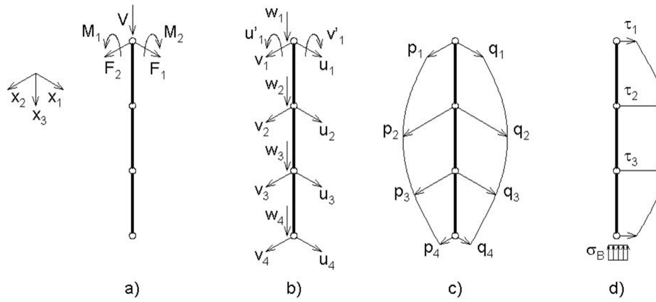

Fig. 2. Model for load lines.

III. LOAD LINES IN THE SOIL

In this work, the reactive tractions from the piles are applied in the soil as load lines. Figure 2 presents the model adopted, with four nodes equally spaced along the pile.

The load lines influence may be computed in Equation (1) with an additional term as follows

$$\mathrm{c_{ij}} u_j + \int_\Gamma p_{ij}^* u_j d\Gamma = \int_\Gamma u_{ij}^* p_j d\Gamma + \sum_{e=1}^{nl} \left[\int_{\Gamma^e} u_{ij}^* s_j^e d\Gamma^e \right] \tag{12}$$

where nl is the number of load lines, Γ^e are their external surface and s_j^e are the tractions presented in Figures 2c and 2d. The tractions are approximated from the nodal values s_j^{ek} using nf polynomial shape functions ϕ:

$$s_j^e = \sum_{k=1}^{nf} \phi^k s_j^{ek} \tag{13}$$

Shape functions are written with a dimensionless coordinate $\xi = {}^{2x_3}/_{L} - 1$, where L is the load line length and x_3 is the vertical global coordinate. One may observe that $-1 \le \xi \le 1$, so the use of Gauss points is facilitated. For the horizontal tractions, illustrated in Figure 2c, $nf = 4$ and the shape functions are:

$$\phi^1 = \frac{1}{16}\left(-9\xi^3 + 9\xi^2 + \xi - 1\right) \tag{14}$$

$$\phi^2 = \frac{1}{16}\left(27\xi^3 - 9\xi^2 - 27\xi + 9\right) \tag{15}$$

$$\phi^3 = \frac{1}{16}\left(-27\xi^3 - 9\xi^2 + 27\xi + 9\right) \tag{16}$$

$$\phi^4 = \frac{1}{16}\left(9\xi^3 + 9\xi^2 - \xi - 1\right) \tag{17}$$

ISBN: 978-988-19253-5-0
ISSN: 2078-0958 (Print); ISSN: 2078-0966 (Online)

For shear tractions in direction x_3, $nf = 3$ and the shape functions are

$$\phi^1 = \frac{1}{8}\left(9\xi^2 - 1\right) \tag{18}$$

$$\phi^2 = \frac{1}{4}\left(-9\xi^2 - 6\xi + 3\right) \tag{19}$$

$$\phi^3 = \frac{1}{8}\left(9\xi^2 + 12\xi + 3\right) \tag{20}$$

Finally, for the base reaction $nf = 1$ and a constant approximation is used. Using the shape functions presented above, the integrals that are not singular may be numerically calculated using Gauss points. The term referent to the load lines becomes singular only when the source point belongs to a load line base which is being integrated. In this case, the integral calculation is analytical.

Writing Equation (12) for all boundary points plus the points defined on each load line, the following system of equations is obtained:

$$[H]\{u\} = [G]\{p\} - [M]\{s\} \tag{21}$$

Matrix $[M]$ is obtained from the integrals calculated for all load lines, and vector $\{s\}$ contains the tractions prescribed for them. As the number of equations is equal to the number of unknowns, the system may be solved obtaining all unknowns.

IV. FEM-BEM COUPLING

Each pile is modeled using a single finite element with polynomial shape functions. Lateral displacements are approximated using fourth degree polynomials $\{\varphi\}$. Vertical displacements and lateral tractions are approximated using third degree polynomials $\{\phi\}$. Vertical tractions are approximated using second degree polynomials $\{\omega\}$ and the tractions at the pile base are considered constant. Using a dimensionless coordinate $\xi = \frac{x_3}{L}$, where x_3 is the global vertical coordinate and L is the pile length, $\{\varphi\}$, $\{\phi\}$ and $\{\omega\}$ may be written as:

$$\{\varphi\} = \left\{ \begin{array}{c} -\frac{99}{4}\xi^4 + 45\xi^3 - \frac{85}{4}\xi^2 + 1 \\ -\frac{9}{2}\xi^4 L + 9\xi^3 L - \frac{11}{2}\xi^2 L + \xi L \\ \frac{81}{2}\xi^4 - \frac{135}{2}\xi^3 + 27\xi^2 \\ -\frac{81}{4}\xi^4 + 27\xi^3 - \frac{27}{4}\xi^2 \\ \frac{9}{2}\xi^4 - \frac{9}{2}\xi^3 + \xi^2 \end{array} \right\} \tag{22}$$

$$\{\phi\} = \left\{ \begin{array}{c} -\frac{9}{2}\xi^3 + 9\xi^2 - \frac{11}{2}\xi + 1 \\ \frac{27}{2}\xi^3 - \frac{45}{2}\xi^2 + 9\xi \\ -\frac{27}{2}\xi^3 + 18\xi^2 - \frac{9}{2}\xi \\ \frac{9}{2}\xi^3 - \frac{9}{2}\xi^2 + \xi \end{array} \right\} \tag{23}$$

$$\{\omega\} = \left\{ \begin{array}{c} \frac{9}{2}\xi^2 - \frac{9}{2}\xi + 1 \\ -9\xi^2 + 6\xi \\ \frac{9}{2}\xi^2 - \frac{3}{2}\xi \end{array} \right\} \tag{24}$$

The next step is obtaining the total potential energy function, considering internal and external contributions. To obtain the final system of equations, such function must be minimized with respect to the nodal parameters. The result is:

$$[K]\{u\} = \{f\} - [Q]\{y\} \rightarrow [K]\{u\} = \{f\} - \{r\} \tag{25}$$

where $[K]$ is the stiffness matrix of the pile, $\{u\}$ contains nodal displacements, $\{f\}$ contains nodal loads, $\{y\}$ contains distributed tractions and $[Q]$ is a matrix that transforms distributed tractions into nodal loads. Therefore, $\{r\}$ contains nodal loads that represent the distributed loads.

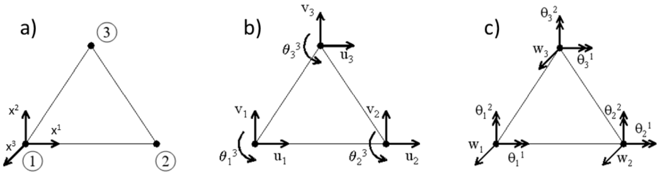

Fig. 3. Triangular finite element.

Now a brief description of the triangular finite element used for the raft and slabs will be presented. The element has three nodes at its vertices as presented in Figure 3a with the local node numbering and a local rectangular system of coordinates x^i, where the superscript i indicates the direction. Each node, indicated with the subscript j, has six degrees of freedom (DOFs). Three of them, u_j, v_j and θ_j^3, may be visualized in Figure 3b which refers to the membrane effects. The other three, w_j, θ_j^1 and θ_j^2, are presented in Figure 3c which refers to the plate effects. In Figure 3c, rotational DOFs are indicated with a double arrow for better visualization. All DOFs of the finite element may be arranged into three vectors, one for each node, as shown below:

$$\begin{array}{l} \{\mathbf{u}_1\}^T = \{\ u_1 \quad v_1 \quad {\theta_1}^3 \quad w_1 \quad {\theta_1}^1 \quad {\theta_1}^2\ \} \\ \{\mathbf{u}_2\}^T = \{\ u_2 \quad v_2 \quad {\theta_2}^3 \quad w_2 \quad {\theta_2}^1 \quad {\theta_2}^2\ \} \\ \{\mathbf{u}_3\}^T = \{\ u_3 \quad v_3 \quad {\theta_3}^3 \quad w_3 \quad {\theta_3}^1 \quad {\theta_3}^2\ \} \end{array} \tag{26}$$

Displacements at any point P of the finite element, with coordinates x_1, x_2 and x_3, may be written as

$$\{\mathbf{u}\} = \left\{ \begin{array}{c} u \\ v \\ w \end{array} \right\} = \left\{ \begin{array}{c} u_0 - x_3 \frac{\partial w_0}{\partial x_1} \\ v_0 - x_3 \frac{\partial w_0}{\partial x_2} \\ w_0 \end{array} \right\} \tag{27}$$

where u_0, v_0, and w_0 are the displacements for the projection of P at the mid plane of the finite element. The strain field may be obtained from the displacements as follows:

$$\{\varepsilon\} = \{\varepsilon_m\} + \{\varepsilon_p\} = \left\{ \begin{array}{c} \frac{\partial u_0}{\partial x_1} \\ \frac{\partial v_0}{\partial x_2} \\ \frac{\partial u_0}{\partial x_2} + \frac{\partial v_0}{\partial x_1} \end{array} \right\} - x_3 \left\{ \begin{array}{c} \frac{\partial^2 w_0}{\partial {x_1}^2} \\ \frac{\partial^2 w_0}{\partial {x_2}^2} \\ 2\frac{\partial^2 w_0}{\partial x_1 \partial x_2} \end{array} \right\} \tag{28}$$

where index m corresponds to the membrane effect and the index p indicates the plate effect. Equation (28) relates the strain field to the displacement field, which may be related to the nodal displacements using the element shape functions. Using these functions and Equation (28), it is possible to relate strains with the DOFs of the finite element as follows:

$$\{\varepsilon\} = [B] \left\{ \begin{array}{c} \mathbf{u}_1 \\ \mathbf{u}_2 \\ \mathbf{u}_3 \end{array} \right\} \tag{29}$$

It is also necessary to relate strains with stresses. For linear elasticity this may be done using a matrix $[D]$ which is obtained from Hooke's law:

$$\{\sigma\} = [D]\{\varepsilon\} \tag{30}$$

ISBN: 978-988-19253-5-0
ISSN: 2078-0958 (Print); ISSN: 2078-0966 (Online)

In the end, the stiffness matrix of the element is obtained by integrating the domain Ω of the element:

$$[K] = \int\limits_{\Omega} [B]^T [D] [B] \, d\Omega \tag{31}$$

More detail about the membrane and plate effects of this element may be consulted in references [21] and [22], respectively.

All finite element contributions, including piles and the raft, are assembled to the same system of equations. This system has the form of Equation (25), which is later used to demonstrate how the FEM/BEM coupling is made. The starting point is Equation (21), which may be rewritten as:

$$[H] \{u\} = [T] \{y\} \tag{32}$$

Matrix $[T]$ contains the terms of matrices $[G]$ and $[M]$ and $\{y\}$ contains the distributed loads of vectors $\{p\}$ and $\{s\}$. Next step is isolating the distributed loads, which are transformed in nodal loads using a matrix $[Q]$.

$$[T]^{-1} [H] \{u\} = \{y\} \rightarrow [B] \{u\} = \{y\} \tag{33}$$

$$[Q] [B] \{u\} = [Q] \{y\} \rightarrow [D] \{u\} = \{r\} \tag{34}$$

Before relating Equations (25) and (34), they must be expanded as to contain all degrees of freedom defined in the coupled FEM-BEM model. The result is

$$\left[\bar{K}\right] \{\bar{u}_{FEM}\} = \{\bar{f}\} - \{\bar{r}_{FEM}\} \tag{35}$$

$$\left[\bar{D}\right] \{\bar{u}_{BEM}\} = \{\bar{r}_{BEM}\} \tag{36}$$

These equations are related by imposing compatibility and equilibrium conditions, which are $\{\bar{u}_{FEM}\} = \{\bar{u}_{BEM}\} = \{\bar{u}\}$ and $\{\bar{r}_{FEM}\} = \{\bar{r}_{BEM}\} = \{\bar{r}\}$. The following expressions are then obtained:

$$\left[\bar{K}\right] \{\bar{u}\} = \{\bar{f}\} - \left[\bar{D}\right] \{\bar{u}\} \tag{37}$$

$$\left(\left[\bar{K}\right] + \left[\bar{D}\right]\right) \{\bar{u}\} = \{\bar{f}\} \tag{38}$$

$$\left[\bar{A}\right] \{\bar{u}\} = \{\bar{f}\} \tag{39}$$

where $\{\bar{u}\}$ contain all unknown displacements of the FEM-BEM model. Once the number of equations is equal to the number of unknowns, the system may be solved obtaining all unknowns.

V. EXAMPLES

A. Piled raft on a layered domain

A raft with nine piles on a layered domain is considered, as presented in Figure 4 with all geometrical and material parameters. Young's module is represented as E, Poisson Ratio as ν and thickness as t. The R subscript indicates the raft, P indicates piles and numbers refer to layers. All piles diameter is $0,5\ m$ and are numbered considering the symmetry planes. The raft is uniformly loaded with $0,04\ MPa$.

Figure 5a contains the mesh used for the surface and contacts, with 160 BEs and 32 IBEs. Figure 5b contains the FE mesh employed for the raft, with the pile positions detached. For piles a one-dimensional FE is used, as previously presented.

Figure 6 presents vertical displacements along the piles, using numbers defined in Figure 4. Pile 3 has the larger

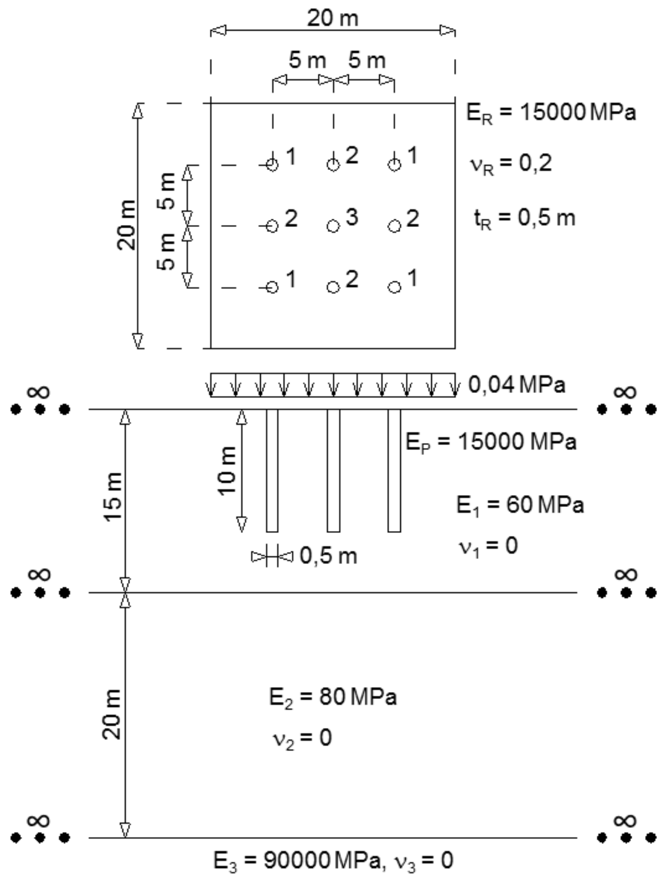

Fig. 4. First example.

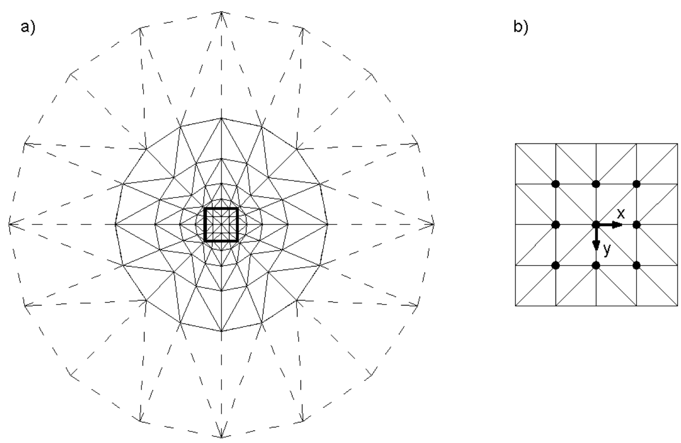

Fig. 5. Mesh employed.

displacements, followed by piles 2 and piles 1 with the smaller ones. The result was also symmetric as expected and the magnitude of the values is coherent. This facts allow to conclude the the values here obtained are trustworthy.

B. Building resting on a layered domain

The objective of this example is to demonstrate the generality of the presented formulation. The problem to be analyzed is presented in Figure 7 and considers a building with its foundations, resting on a layered media. In Figure 7a the lateral view is illustrated, Figure 7b contains the standard

ISBN: 978-988-19253-5-0
ISSN: 2078-0958 (Print); ISSN: 2078-0966 (Online)

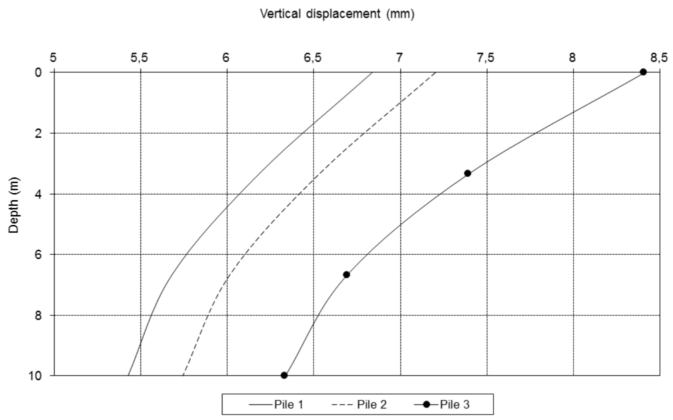

Fig. 6. Displacements for distributed load.

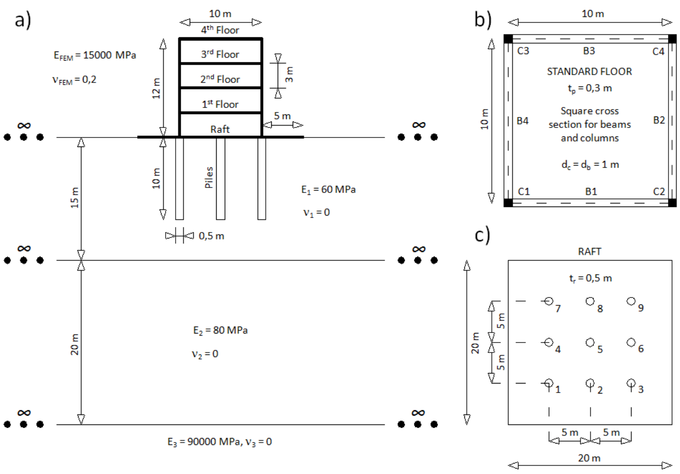

Fig. 7. Soil-building interaction

floor considered and in Figure 7c is presented the top view of the structural foundations included.

The Poisson Ratio is zero for all soil layers. The elasticity modulus of the layers is 60 MPa for the top one, 80 MPa for the second and 90000 MPa for the base layer. The thickness is 15 m for the top layer, 20 m for the second and the base layer is considered infinite. The diameter of all piles is $0,5$ m, their length is 10 m and they are spaced of 5 m. The square raft has size 20 m and thickness $0,5$ m. The elasticity modulus of all materials modeled with the FEM is 15000 MPa and their Poisson ratio is $0,2$. This includes all piles, beams, columns, slabs and the raft.

The building has four floors, as shown in Figure 7a. All floors have the same standard geometry, as presented in Figure 7b, with a slab with thickness $0,3$ m, four beams supporting this slab and four columns supporting the beams. A square cross section size 1 m is used for all beams and columns. The base of each column is connected to the raft at the same node where a corner pile is connected. Corner piles are numerated in Figure 7c as 1, 3, 7 and 9.

Figure 8 presents the FE-BE-IBE mesh employed in the example. Figure 8a contains the top view of the mesh used for the soil surface and contacts between layers, totalizing 480 BEs and 96 IBEs. The square detached at the center indicates the position of the raft at the surface. In Figure 8b is illustrated the mesh with 32 FEs used for the raft,

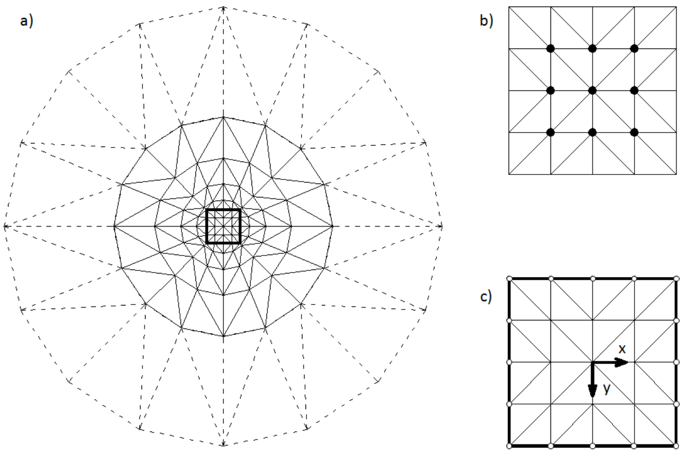

Fig. 8. FE/BE/IBE mesh employed

together with the position of the piles. Finally, Figure 8c contains the 32 FE mesh used for the slabs. Lines detached at the boundary indicate the FEs used for beams, totalizing 16 FEs for each floor. Furthermore, each part of the columns between floors is divided into 4 FEs. Considering all floors plus the raft, the total number of two-dimensional FEs is 160 and the total of one-dimensional FEs is 128.

Piles are also simulated with the FEM, employing the FE with 14 parameters presented previously. The axis of any pile is orthogonal to the surface of the soil.

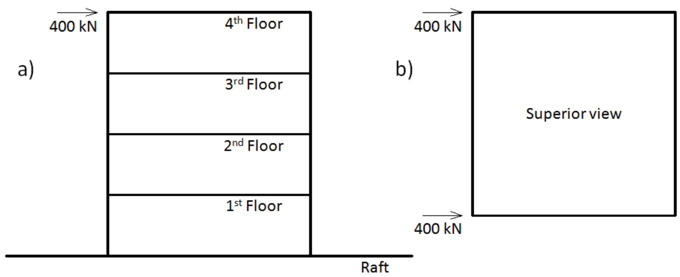

Fig. 9. Horizontal loads applied

Two horizontal forces are applied at lateral points of the building, as shown in Figure 9. In Figure 9a is presented a lateral view of the structure, with the external forces contained in the plane of the fourth floor. Figure 9b shows a top view, where the position of the forces may be visualized from another perspective.

Considering these loads, Figure 10 contains the horizontal displacements calculated for column $C1$, which position may be observed in Figure 7b. In this case two simulations were also performed, one considering the flexible base illustrated in Figure 7a and another considering a rigid base. The rigid base was represented restraining displacements at the base node of all columns.

As expected, the column presents higher displacements when the elastic foundation is considered. For the rigid base the horizontal displacement calculated for the top of column $C1$ was $8,9$ mm, and for the elastic foundation this value increased to $11,3$ mm. Furthermore, analyzing displacements along the column in both cases, it may be concluded that it becomes more inclined when the elastic foundation is considered. Horizontal displacements combined with vertical loads

ISBN: 978-988-19253-5-0
ISSN: 2078-0958 (Print); ISSN: 2078-0966 (Online)

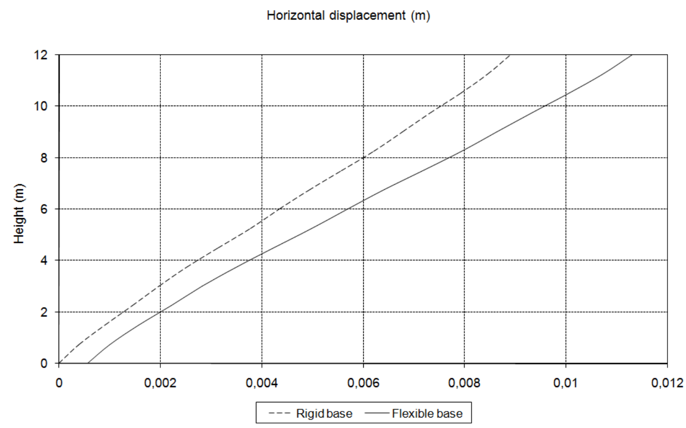

Fig. 10. Horizontal displacement of column $C1$

may produce moments that cannot be unvalued and could compromise the safety of the structure. This demonstrates that it is important to include the flexibility of the foundations when projecting buildings.

VI. CONCLUSIONS

In this paper a formulation for building-soil interaction analysis was presented. The FEM/BEM equations together with the techniques from references [17], [18] contributed with reducing the total number of degrees of freedom. Piles are modeled using one-dimensional FEs, whose influence in the soil is computed by integrating load lines. Two examples were presented. In both of them the results obtained were considered coherent. In the end, it may be concluded that the presented formulation is a powerful and attractive alternative for soil-structure interaction analysis.

ACKNOWLEDGEMENTS

Thanks are due to the research council FAPESP and the University of São Paulo.

REFERENCES

[1] Basu, D., Prezzi, M., Salgado, R. and Chakraborty, T. Settlement analysis of piles with rectangular cross sections in multi-layered soils, *Comput. Geotech.* (2008) **35**:563–575.

[2] Shahmohamadi, M., Khojasteh, A., Rahimian, M. and Pak, R.Y.S. Axial soil-pile interaction in a transversely isotropic half-space, *Int. J. Eng. Sci.* (2011) **49**:934–949.

[3] Georgiadis, K., Georgiadis, M. and Anagnostopoulos, C. Lateral bearing capacity of rigid piles near clay slopes, *Soils. Found.* (2013) **53**:144–154.

[4] Clouteau, D., Cottereau, R. and Lombaert, G. Dynamics of structures coupled with elastic media - A review of numerical models and methods, *J. Sound Vib.* (2013) **332**:2415–2436.

[5] Kim, Y. and Jeong, S. Analysis of soil resistance on laterally loaded piles based on 3D soilpile interaction, *Comput. Geotech.* (2011) **38**:248–257.

[6] Bourgeois, E., de Buhan, P. and Hassen, G. Settlement analysis of piled-raft foundations by means of a multiphase model accounting for soil-pile interactions, *Comput. Geotech.* (2012) **46**:26–38.

[7] Su, D. and Li, J.H. Three-dimensional finite element study of a single pile response to multidirectional lateral loadings incorporating the simplified state-dependent dilatancy model, *Comput. Geotech.* (2013) **50**:129–142.

[8] Peng, J.R., Rouainia, M. and Clarke, B.G. Finite element analysis of laterally loaded fin piles, *Comput. Struct.* (2010) **88**:1239–1247.

[9] Ai, Z.Y. and Cheng, Y.C. Analysis of vertically loaded piles in multi-layered transversely isotropic soils by BEM, *Eng. Anal. Bound. Elem.* (2013) **37**:327–335.

[10] Matos Filho, R., Mendonça, A.V. and Paiva, J.B. Static boundary element analysis of piles submitted to horizontal and vertical loads, *Eng. Anal. Bound. Elem.* (2005) **29**:195–203.

[11] Masoumi, H.R., Degrande, G. and Lombaer, G. Prediction of free field vibrations due to pile driving using a dynamic soilstructure interaction formulation, *Soil Dyn. Earthq. Eng.* (2007) **27**:126–143.

[12] Padron, L.A., Aznarez, J.J. and Maeso O. 3-D boundary elementfinite element method for the dynamic analysis of piled buildings, *Eng. Anal. Bound. Elem.* (2011) **35**:465–477.

[13] Almeida, V.S. and Paiva, J.B. Static analysis of soil/pile interaction in layered soil by BEM/BEM coupling, *Adv. Eng. Softw.* (2007) **38**:835–845.

[14] Millan, M.A. and Dominguez, J. Simplified BEM/FEM model for dynamic analysis of structures on pile sand pile groups in viscoelastic and poroelastic soils, *Eng. Anal. Bound. Elem.* (2009) **33**:25–34.

[15] Elahi, H., Moradi, M., Poulos, H.G. and Ghalandarzadeh, A. Pseudo-static approach for seismic analysis of pile group, *Comput. Geotech.* (2010) **37**:25–39.

[16] Kucukarslan, S., Banerjee, P.K. and Bildik, N. Inelastic analysis of pile soil structure interaction, *Eng. Struct.* (2003) **25**:1231–1239.

[17] Ribeiro, D.B. and Paiva, J.B. An alternative multi-region BEM technique for three-dimensional elastic problems, *Eng. Anal. Bound. Elem.* (2009) **33**:499–507.

[18] Ribeiro, D.B. and Paiva, J.B. Analyzing static three-dimensional elastic domains with a new infinite boundary element formulation, *Eng. Anal. Bound. Elem.* (2010) **34**:707–713.

[19] Guiggiani, M. and Gigante, A. A general algorithm for multidimensional cauchy principal value integrals in the boundary element method, *J. Appl. Mech.* (1990) **57**:906–915.

[20] Moser, W., Duenser, C. and Beer, G. Mapped infinite elements for three-dimensional multi-region boundary element analysis, *Int. J. Numer. Meth. Eng.* (2004) **61**:317–328.

[21] Bergan, P.G. and Felippa, C.A. A triangular membrane element with rotacional degrees of freedom, *Comput. Method. Appl. M.* (1985) **50**:25–69.

[22] Batoz, J.L. A study of tree-node triangular plate bending elements, *Int. J. Numer. Meth. Eng.* (1980) **15**:1771–1812.

[23] Wardle, L.J. and Fraser, R.A. Finite element analysis of a plate on a layered cross-anisotropic foundation, in "Proceedings of the First International Conference of Finite Element Methods in Engineering" (1974) University of New South Wales, Australia, 565–578.

[24] Fraser, R.A. and Wardle, L.J. Numerical analysis of rectangular rafts on layered foundations, *Geotechnique* (1976) **26**:613–630.

[25] Wang, Y.H., Tham, L.G., Tsui, Y. and Yue, Z.Q. Plate on layered foundation analyzed by a semi-analytical and semi-numerical method, *Comput. Geotech.* (2003) **30**:409–418.

ISBN: 978-988-19253-5-0
ISSN: 2078-0958 (Print); ISSN: 2078-0966 (Online)